Title

Identification of tumorigenic cells and therapeutic targets in pancreatic neuroendocrine tumors

Journal

Proceedings of the National Academy of Sciences of the United States of America, 113(16)

ISSN

0027-8424

Authors

Krampitz, Geoffrey Wayne
George, Benson M
Willingham, Stephen B
et al.

Publication Date

2016-04-19

DOI

10.1073/pnas.1600007113

Peer reviewed

Identification of tumorigenic cells and therapeutic targets in pancreatic neuroendocrine tumors

Geoffrey Wayne Krampitz[a,b,c,1], Benson M. George[b,c], Stephen B. Willingham[b,c], Jens-Peter Volkmer[b,c], Kipp Weiskopf[b,c], Nadine Jahchan[b,d,e,2], Aaron M. Newman[b,c], Debashis Sahoo[b,c,3], Allison J. Zemek[f], Rebecca L. Yanovsky[b,c], Julia K. Nguyen[b,c], Peter J. Schnorr[b,c], Pawel K. Mazur[b,d,e], Julien Sage[b,d,e], Teri A. Longacre[f], Brendan C. Visser[a], George A. Poultsides[a], Jeffrey A. Norton[a,c], and Irving L. Weissman[b,c,f,1]

[a]Department of Surgery, Stanford University School of Medicine, Stanford, CA 94305; [b]Institute of Stem Cell Biology and Regenerative Medicine, Stanford University School of Medicine, Stanford, CA 94305; [c]Ludwig Center for Cancer Stem Cell Research and Medicine, Stanford University, Stanford, CA 94305; [d]Department of Pediatrics, Stanford University School of Medicine, Stanford, CA 94305; [e]Department of Genetics, Stanford University School of Medicine, Stanford, CA 94305; and [f]Department of Pathology, Stanford University School of Medicine, Stanford, CA 94305

Contributed by Irving L. Weissman, January 27, 2016 (sent for review December 21, 2015; reviewed by Ed Harlow, Luis F. Parada, Jeremy N. Rich, and Owen N. Witte)

Pancreatic neuroendocrine tumors (PanNETs) are a type of pancreatic cancer with limited therapeutic options. Consequently, most patients with advanced disease die from tumor progression. Current evidence indicates that a subset of cancer cells is responsible for tumor development, metastasis, and recurrence, and targeting these tumor-initiating cells is necessary to eradicate tumors. However, tumor-initiating cells and the biological processes that promote pathogenesis remain largely uncharacterized in PanNETs. Here we profile primary and metastatic tumors from an index patient and demonstrate that MET proto-oncogene activation is important for tumor growth in PanNET xenograft models. We identify a highly tumorigenic cell population within several independent surgically acquired PanNETs characterized by increased cell-surface protein CD90 expression and aldehyde dehydrogenase A1 (ALDHA1) activity, and provide in vitro and in vivo evidence for their stem-like properties. We performed proteomic profiling of 332 antigens in two cell lines and four primary tumors, and showed that CD47, a cell-surface protein that acts as a "don't eat me" signal co-opted by cancers to evade innate immune surveillance, is ubiquitously expressed. Moreover, CD47 coexpresses with MET and is enriched in CD90^{hi} cells. Furthermore, blocking CD47 signaling promotes engulfment of tumor cells by macrophages in vitro and inhibits xenograft tumor growth, prevents metastases, and prolongs survival in vivo.

pancreatic neuroendocrine tumor | CD47 | CD90 | MET | cancer stem cell

Pancreatic neuroendocrine tumors (PanNETs) are a heterogeneous group of neoplasms that constitute between 3% and 5% of all pancreatic malignancies (1). Despite recent advances in medical treatments (2, 3), complete surgical resection is the only curative therapy for PanNET patients with localized tumors and limited metastases (4). There is a critical need to characterize the biological processes and molecular mechanisms that initiate PanNETs, drive their progression, and allow them to evade therapy to facilitate the development of novel treatments for patients with these tumors.

A model of cancer in which neoplasms are dependent on a subset of tumorigenic cells that are responsible for initiation, maintenance, and propagation of tumors has been proposed previously (5). These cancer stem cells are defined by their ability to self-renew, differentiate into the heterogeneous cell populations comprising the tumor, and the ability to develop new neoplasms when transplanted into immunodeficient mice (5). These rare cell populations, identified by their unique cell-surface antigen repertoire, were first characterized in acute myelogenous leukemia and were shown to fully recapitulate the disease in mice (6). Subsequently, tumor-initiating cells were isolated in solid tumors (7–9). Previous experimental evidence indicates that effectively curing cancers requires eradicating the tumor-initiating cell pool (5). However, tumor-initiating cells have yet to be identified in PanNETs, preventing the development of desperately needed therapies.

Cancer cells can evade immune surveillance, inhibit immune effector cell function, and even co-opt immune cells to support their growth and metastasis (10). Generally, the immune system monitors the body, looking to destroy malignant cells before they form malignant neoplasms (11). Significant cancer immunology research has emerged to determine the precise mechanisms that enable immune evasion, with the goal of developing strategies that immunologically "unmask" these cells.

CD47 is highly expressed on the surface of cells in all tested cancers and functions as a negative regulator of macrophage-mediated phagocytosis. CD47 binds signal regulatory protein alpha (SIRPα) on macrophages, which activates SHP-1 tyrosine phosphatases that function to inhibit cytoskeletal rearrangements

Significance

This is the first in-depth profiling of pancreatic neuroendocrine tumors (PanNETs), to our knowledge, that illuminates fundamental biological processes for this class of tumors. Beginning with the index case and confirmed with additional patient tumors, we showed the dependence on paracrine signaling through the hepatocyte growth factor (HGF)/receptor tyrosine kinase MET axis. We created a novel cell line derived from a well-differentiated PanNET with autocrine HGF/MET signaling. We also identified the cell-surface protein CD90 as a marker of the tumor-initiating cell population in PanNETs that allows for prospective isolation of this critical cell population. Finally, we demonstrated the efficacy of anti-CD47 therapy in PanNETs. These findings provide a foundation for developing therapeutic strategies that eliminate tumor-initiating cells in PanNETs and show how deep examination of individual cases can lead to potential therapies.

Author contributions: G.W.K., J.A.N., and I.L.W. designed research; G.W.K., B.M.G., S.B.W., J.-P.V., K.W., N.J., A.M.N., D.S., A.J.Z., R.L.Y., J.K.N., P.J.S., and I.L.W. performed research; G.W.K., B.M.G., J.-P.V., K.W., N.J., A.M.N., D.S., A.J.Z., P.K.M., J.S., T.A.L., B.C.V., G.A.P., and I.L.W. contributed new reagents/analytic tools; G.W.K., B.M.G., S.B.W., J.-P.V., K.W., N.J., A.M.N., D.S., A.J.Z., R.L.Y., J.K.N., P.J.S., J.A.N., and I.L.W. analyzed data; and G.W.K., B.M.G., S.B.W., J.A.N., and I.L.W. wrote the paper.

Reviewers: E.H., Harvard Medical School; L.F.P., Memorial Sloan-Kettering Cancer Center; J.N.R., Cleveland Clinic; and O.N.W., Howard Hughes Medical Institute and University of California, Los Angeles.

The authors declare no conflict of interest.

Data deposition: The sequences reported in this paper have been deposited in the Sequence Read Archive (SRA) database, www.ncbi.nlm.nih.gov/traces/sra (accession no. SRS1283061).

[1]To whom correspondence may be addressed. Email: krampitz@stanford.edu or irv@stanford.edu.

[2]Present address: ORIC Pharmaceuticals, South San Francisco, CA 94080.

[3]Present address: Departments of Pediatrics and Computer Science and Engineering, University of California, San Diego, La Jolla, CA 92093.

This article contains supporting information online at www.pnas.org/lookup/suppl/doi:10.1073/pnas.1600007113/-/DCSupplemental.

necessary for phagocytosis, thus functioning as a "don't eat me" signal. Notably, expression of CD47 among tumor cells is often highest in the tumor-initiating cell population, suggesting their dependence on CD47 expression to prevent phagocytic elimination by innate immune cells (11). Blocking the CD47–SIRPα interaction allows phagocytes to effectively destroy cancer cells in vitro and in vivo, leading to inhibition or elimination of primary tumors and metastases in human cancer xenotransplantation models (12). Furthermore, we have shown that blocking CD47 with monoclonal antibodies and other agents can dramatically enhance the efficacy of cancer-targeting monoclonal antibodies, including rituximab (anti-CD20) for lymphoma and trastuzumab (anti-her2) for breast cancer (13, 14). In addition, we have shown that the anti-CD47 antibody treatment selectively increases the ability of macrophages to prime and activate cytotoxic T lymphocytes, which may limit tumor growth beyond the time of anti-CD47 monoclonal antibody treatment (15).

These considerations prompted us to identify tumor-initiating cells and explore mechanisms by which tumors propagate and evade immune surveillance. Here we report a signaling pathway critical for PanNET growth in immunodeficient mice. We also developed a cell line and reproducible xenograft models derived from a patient PanNET, the lack of which have previously been major limitations in the study of PanNETs. We further identified several cell-surface proteins expressed on the PanNET-initiating cells, and characterized the enzymatic and genetic properties of tumor-initiating cells in PanNETs. Furthermore, we profiled the cell-surface protein repertoire of PanNET cells and revealed a number of potential therapeutic targets with functional significance. We validated these targets using in vitro phagocytosis assays, and demonstrated the efficacy of anti-CD47 monoclonal antibody therapy on PanNET growth using a genetic mouse model of PanNETs as well as xenograft assays of patient-derived PanNETs. These results provide preclinical evidence that anti-CD47 therapy may improve outcomes for patients with PanNETs, and also validate an approach of studying a selected subset of index cases of cancer to make generalizable progress.

Results

In an Index Case, MET Activation Is Critical for Tumor Growth in Mouse Xenograft Models. We began with an extended multidisciplinary analysis of an index patient who made tissues available for analysis at several points in the disease course (tumors 1a and 1b; Dataset S1). We used RNA and genomic sequencing to profile the patient's primary tumor and lymph node metastasis (Fig. S1*A*). Bioinformatic analysis of the gene expression profiles was used to identify genes potentially involved in the tumorigenic process. We used a previously described method for extracting Boolean implications (if–then relationships) between genes with publicly available gene expression microarray data for all human tissue (normal and cancer alike) (Dataset S2) as controls. We then superimposed the gene expression microarray data of our index patient's primary tumor and adjacent, noncancerous pancreatic tissue (16).

We noted that *MET* was highly expressed on the primary tumor, whereas the gene that encodes the protein MET ligand, hepatocyte growth factor (HGF), was not expressed in the tumor but was instead expressed in the adjacent, noncancerous tissue (Fig. 1*A*). *MET* is a gene encoding a receptor tyrosine kinase normally expressed during wound healing and on stem and progenitor cells during embryonic development, and is a proto-oncogene that can be expressed in invasive cancers (17). We also found that *CD47* was highly expressed on the primary tumor compared with surrounding noncancerous pancreatic tissue (Fig. 1*B*). Using immunofluorescence staining, we confirmed the coexpression of the neuroendocrine tumor marker chromogranin A (CHGA) and MET in the patient's liver metastasis and lymph node metastasis (Fig. 1 *C* and *D*). Next, we found that cells expressing CHGA in both metastatic sites did not simultaneously express HGF (Fig. 1 *E* and *F*). However, clusters of cells in tumor-adjacent normal liver and pancreas tissue expressed HGF

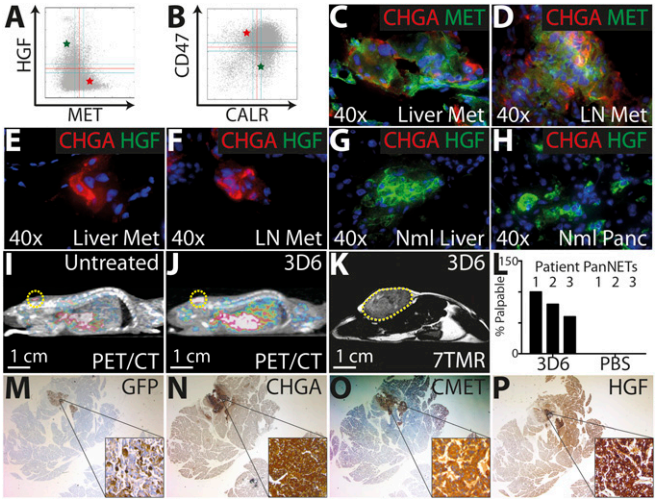

Fig. 1. MET activation is critical for tumor growth in mouse xenograft models. (*A* and *B*) Boolean implication analysis of the index patient tumor showing the relationships between pairs of gene expression of prospective therapeutic targets *HGF* and *MET* (*A*) and *CD47* and *CALR* (*B*). Each point in the scatter plot corresponds to a microarray experiment, where the two axes correspond to the expression levels of two genes. The patient primary tumor (red stars), adjacent normal pancreas (green stars), and other human tissue samples (gray dots) are represented, and threshold values for high and low (red lines) and intermediate (green lines) gene expression using the BooleanNet algorithm (16). (*C*–*F*) Immunofluorescence staining of the patient's liver and lymph node metastases. Costaining of the neuroendocrine tumor marker CHGA and MET in the patient's liver metastasis (*C*) and lymph node (LN) metastasis (*D*). Costaining of the neuroendocrine tumor marker CHGA and HGF in the patient's liver metastasis (*E*) and lymph node metastasis (*F*). (*G* and *H*) Costaining of the neuroendocrine tumor marker CHGA and HGF in the patient's normal (Nml) liver (*G*) and normal pancreas (*H*). (*I*) Positron-emission tomography/computed tomography (PET/CT) showing DNA synthetic activity in a patient lymph node metastasis tumor fragment (yellow outline) 6 mo after transplantation s.c. into the dorsum of an NSG mouse. (*J*) PET/CT showing increased DNA synthetic activity in the tumor fragment (yellow outline) in a mouse treated with 3D6 (Genentech), an agonist antibody for MET. (*K*) Sagittal section of a T2-weighted, spin-echo sequence, 7-T magnetic resonance image showing a tumor xenograft (yellow outline) that developed in the mouse 1 mo after initiating treatment with 3D6 antibody. (*L*) PanNET fragments from three other primary patient tumors that previously did not grow in NSG mice had increased engraftment efficiency when treated with 3D6 compared with PBS vehicle control. PanNET cells derived from a primary patient tumor with autocrine MET stimulation were able to engraft when injected orthotopically into NSG mice without exogenous MET activation. Twenty-five thousand luciferase-labeled APL1 cells were injected orthotopically into the pancreases of NSG mice and allowed to engraft for 2 wk before immunohistochemical analysis. (*M*) Tumor engraftment was confirmed by the presence of GFP-expressing cells in the pancreases of these mice. (*N*) GFP-positive cells corresponded to cells expressing the PanNET marker chromogranin A. (*O* and *P*) APL1 tumors expressed MET (*O*) and HGF (*P*), allowing for autocrine MET signaling.

(Fig. 1 *G* and *H*). Similarly, we confirmed coexpression of CHGA and CD47 in the two metastatic sites (Fig. S1 *F* and *G*). DNA sequencing of the primary index patient tumor in the pancreas revealed no mutations in the MET coding or intronic regions [National Center for Biotechnology Information (NCBI) Sequence Read Archive (SRA) sample accession no. SRS1283061]; therefore, we sought to test whether paracrine HGF was important for PanNET growth.

Primary tumor fragments from the index patient's lymph node metastasis were s.c. transplanted into NOD scid gamma (NSG) mice, but the tumor xenografts failed to grow after 6 mo (Fig. 1*I*). Because mouse HGF does not activate the human MET receptor (18), we treated the mice with 3D6, a humanized monoclonal antibody agonist for MET (Genentech). Upon stimulation of MET

signaling, the tumor fragments showed a significant increase in uptake of the deoxythymidine analog ^{18}F-labeled 3′-deoxy-3′-fluorothymidine ([^{18}F]FLT), a measure of cellular proliferation (Fig. 1*J*). Continued administration of 3D6 enabled the formation of a large xenograft tumor (Fig. 1*K*). To determine whether MET stimulation was necessary for growth in other patient tumors, we s.c. transplanted three other patient PanNET fragments, which did not grow without exogenous MET activation, into the backs of NSG mice. We found that mice treated with 3D6 developed palpable tumors with an average of 80% efficiency but that mice treated with PBS control did not grow tumors at all (Fig. 1*L*). Thus, MET stimulation with 3D6 significantly increased the transplantation efficiency of multiple patient PanNET samples. We next tested whether expression of MET on PanNETs has any clinical significance. We stained and scored a tissue microarray for expression of MET (Fig. S2 *A–D*) and found that high expression of MET on tumors correlated with decreased survival (Fig. S3*D*).

We transplanted fragments from 39 distinct well-differentiated, World Health Organization (WHO) grade 1 and 2 patient PanNETs (Dataset S1) into NSG mice. Only one of these tumors (tumor 2; Dataset S1) generated xenografts in over 90% of NSG mice over multiple passages. From this patient tumor, we developed a PanNET cell line, APL1, capable of growing in vitro and in vivo. We injected APL1 cells expressing a GFP-luciferase fusion protein (APL1-GFP-Luc) orthotopically into NSG mice. Tumor engraftment was confirmed by staining for GFP expression in the mouse pancreas (Fig. 1*M*). The APL1-GFP-Luc cells expressed human CHGA (Fig. 1*N*), human MET (Fig. 1*O*), and human HGF (Fig. 1*P*). The presence of both MET and HGF in APL1 cells suggests autocrine stimulation, further supporting the importance of MET signaling for tumor growth. In addition, APL1 tumors appeared to be nonfunctional, as they did not express somatostatin (Fig. S3*E*), insulin (Fig. S3*F*), glucagon (Fig. S3*G*), or gastrin (Fig. S3*H*), consistent with the primary patient tumor from which the cells were derived.

Taken together, these data indicate that MET signaling via HGF could be a clinically significant factor governing PanNET growth. Whereas others have shown the importance of MET in PanNET aggressiveness using mouse models and cell lines (19), we were able to demonstrate this using human samples.

CD90 Expression Characterizes Tumor-Initiating Cells in PanNETs. Tumor cells often co-opt stem and progenitor cell properties such as self-renewal, survival, differentiation, migration, and chemoresistance (5). The potential functional conservation of cell-surface and intrinsic enzymatic markers found on self-renewing cells can facilitate identifying tumorigenic cells within heterogeneous tumor masses. To characterize the cellular composition of PanNETs, we analyzed the expression of cell-surface markers common to tumorigenic cells in other cancers. Flow cytometry analysis of patient-derived tumors revealed that CD90 expression was limited to a small subset of PanNET cells, thus segregating tumor cells into two distinct populations (Fig. 2*A* and Fig. S4 *A* and *B*). CD90 (Thy-1) is a glycophosphatidylinositol (GPI)-anchored cell-surface protein present on normal mouse and human hematopoietic stem cells (20) and tumor-initiating cells in several solid tumors (9, 21). Aldehyde dehydrogenase A1 (ALDHA1), an enzyme preferentially expressed in stem and progenitor cells in several tissue types and species (22), was previously detected in neuroendocrine tumor cell lines with anchorage-independent growth potential and increased tumorigenicity in vivo (23). We found that CD90^{hi} PanNET cells demonstrated enhanced expression of ALDHA1 compared with CD90^{neg} cells (Fig. 2*B*), further supporting that CD90^{hi} expression characterizes tumorigenic cells within PanNETs.

To further discern these two major cellular populations within PanNETs, we used fluorescence-activated cell sorting (FACS) to purify cells from the index patient on the basis of CD90 expression. We extracted RNA from the purified tumor cells and performed high-throughput RNA sequencing. Whole-transcriptome analysis revealed over 3,000 differentially expressed genes between CD90^{hi} and CD90^{neg} cells (Dataset S3). Importantly, genes for markers that characterize tumorigenic cells in a number of cancers were differentially expressed (Fig. S4*D*). To functionally annotate each population of cells, we performed gene set enrichment analysis (GSEA). Compared with CD90^{neg} cells, CD90^{hi} cells showed a significant enrichment of genes up-regulated in mammary stem cells, adipose stem cells, and migratory cells (Fig. S4 *E–G*). Moreover, compared with CD90^{neg} cells, CD90^{hi} cells showed a significant enrichment of genes down-regulated in mammary stem cells and genes up-regulated in mature mammary luminal cells and in breast cancer luminal versus mesenchymal cells (Fig. S4 *H–J*). Taken together, these data provide evidence that CD90^{hi} cells have enzymatic and genetic signatures that more closely resemble that of stem and progenitor cells.

We next investigated the ability of CD90 expression to distinguish tumorigenic cells within PanNETs. We FACS-purified cell populations from the original tumor 2 (Dataset S1), which expresses both HGF and MET and is the origin of the APL1 line, based on CD90 expression (Fig. 2*A*). NSG mice injected with 1,000 CD90^{hi} cells developed large xenograft tumors, whereas an equivalent number of CD90^{neg} cells were unable to form tumors (Fig. 2*C*). CD90^{hi} cells also had increased tumorigenic potential compared

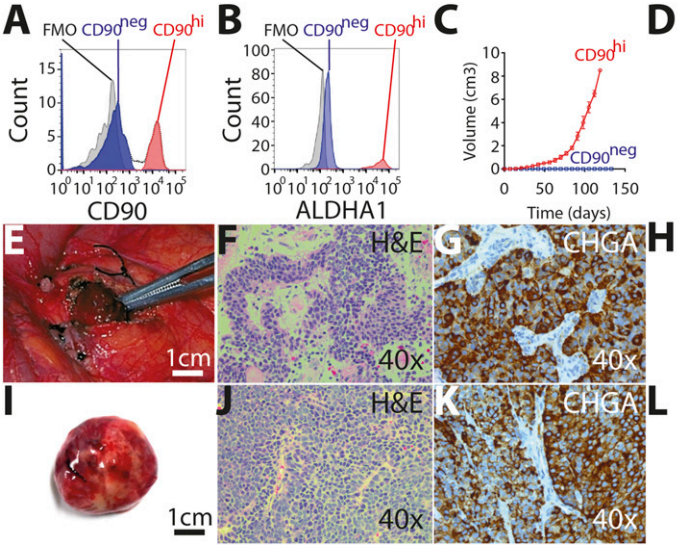

Fig. 2. CD90^{hi} expression characterizes tumor-initiating cells in PanNETs. (*A* and *B*) Flow cytometry analysis of a primary patient tumor showed that CD90 expression is limited to a subset of PanNET cells (*A*) and that PanNET tumorigenicity marker ALDHA1 activity is enhanced in CD90^{hi} cells compared with CD90^{neg} cells (*B*). (*C*) One thousand FACS-purified CD90^{hi} primary PanNET cells injected into NSG mice gave rise to tumors, whereas an equal number of CD90^{neg} cells did not. Means ± SEM. (*D*) Limiting dilution assay showing increased tumorigenic potential of CD90^{hi} compared with CD90^{neg} cells and unsorted cells when injected into NSG mice. (*E–L*) Primary patient tumors (*E–H*) resemble tumor xenografts derived from CD90^{hi} cells injected into NSG mice (*I–L*). Xenografts recapitulate the gross appearance (*I*) and histological features (*J*), express CHGA (*K*), and differentiate into the CD90^{neg} population of cells (*L*) seen in the original tumor (*E–H*). Fluorescence Minus One (FMO) is a type of negative control for flow cytometry using multiple fluorochromes.

with CD90^{neg} and unsorted cells when injected into NSG mice (P = 1.44e-30) (Fig. 2*D*). The increased tumorigenicity of CD90^{hi} cells persisted over multiple passages (P = 0.011) (Dataset S4). Limiting dilution analysis (24) showed a tumor-initiating cell frequency of 1 in 392 for CD90^{hi} cells, 1 in 251,582 for CD90^{neg} cells, and 1 in 9,511 for unsorted cells (Dataset S4). Interestingly, the intraoperative gross appearance of the primary patient sample (Fig. 2*E*) was similar to the gross appearance of a tumor xenograft derived from FACS-purified CD90^{hi} cells (Fig. 2*I*). At the cellular level, hematoxylin and eosin staining of the tumor derived from CD90^{hi} cells (Fig. 2*J*) was indistinguishable from the primary patient tumor (Fig. 2*F*). CHGA was present in secretory granules in the cytoplasm of cells in the primary patient tumor and the xenograft derived from CD90^{hi} cells (Fig. 2 *G* and *K*, respectively). Furthermore, like the primary tumor, the xenograft tumor derived from FACS-purified CD90^{hi} cells gave rise to both CD90^{hi} and CD90^{neg} cells (Fig. 2 *H* and *L*). Taken together, these data indicate that CD90 expression characterizes highly tumorigenic cancer stem cells in PanNETs, and that tumors derived from CD90^{hi} cells recapitulate the composition of the primary patient tumor, including differentiation into CD90^{neg} cells.

Proteomic Analysis Reveals Potential Therapeutic Targets Validated with in Vitro Phagocytosis Assays. To further illuminate the cell-surface repertoire of PanNETs, we performed high-throughput flow cytometry analysis of four additional primary patient PanNETs (tumors 3, 14, 17, and 21; Dataset S1), the BON neuroendocrine tumor cell line, and APL1 cells. The details of this experiment are shown in *Supporting Information* (Fig. S5*A* and Dataset S5). CD47 expression was confirmed on all PanNET cells by flow cytometry analysis (Fig. S5 *B* and *D*) and immunofluorescence (Fig. S5*C*). Furthermore, we found that the tumorigenic CD90^{hi} cells exhibited increased expression of CD47 compared with CD90^{neg} cells (Fig. S5*E*). We stained and scored a tissue microarray for expression of CD47 (Fig. S2 *E–H*) and found that high expression of CD47 on tumors correlated with decreased survival (Fig. S5*F*). These results revealed a number of functionally significant cell-surface proteins for therapeutic targeting, in particular CD47.

Next, we used an in vitro phagocytosis assay to test whether monoclonal antibodies specific to the proteins identified from our analysis could stimulate macrophages to phagocytose human PanNET cells. The details of this experiment are shown in *Supporting Information* (Fig. S5 *G–I*). Antibodies to CD47 (Hu5F9-G4), CD59, and CD147 enhanced engulfment of BON cells by mouse macrophages compared with PBS control (Fig. S5*I*). However, antibodies to CD90, CD63, and EpCAM did not significantly increase phagocytosis of BON tumor cells by mouse macrophages compared with PBS control. Blocking CD47 signaling using monoclonal antibodies (mouse B6H12 or humanized Hu5F9-G4) or a recombinant high-affinity SIRPα variant fused to a human IgG4 Fc fragment (CV1-G4) (14) significantly increased phagocytosis of BON tumor cells by human macrophages (Fig. S5*I*). Moreover, an anti-CD99 antibody alone or in combination with a recombinant high-affinity SIRPα variant (CV1) monomer also induced robust phagocytosis of BON tumor cells by human macrophages (Fig. S5*I*). However, CV1 monomer alone, antibodies against CD90 or MET, or a combination of antibodies against CD90 or MET with CV1 did not significantly increase phagocytosis of BON tumor cells by human macrophages (Fig. S5*I*). Antibodies to CD47 (Hu5F9-G4) and epidermal growth factor receptor (EGFR) (cetuximab, IgG1) induced engulfment of APL1 tumor cells by human macrophages compared with PBS control (Fig. S5*I*). Combinations of Hu5F9-G4 with cetuximab, panitumumab (anti-EGFR, IgG1), or anti-EpCAM antibodies were efficacious as well. However, neither panitumumab nor anti-EpCAM antibodies used alone showed a significant increase in phagocytosis of APL1 tumor cells by human macrophages (Fig. S5*I*).

We have previously shown that cancer cells that have up-regulated CD47 evade immune surveillance, and that blocking CD47 signaling eradicates a number of different tumors in animal models by facilitating programmed cell removal by macrophages (12, 25). However, the expression of CD47, as well as either the in vitro or in vivo efficacy of anti-CD47 monoclonal antibody therapy, in PanNETs has not been described.

Anti-CD47 Therapy Inhibits Tumor Growth, Prevents Metastases, and Prolongs Survival in Vivo. Because anti-CD47 monoclonal antibody treatment induced the phagocytosis of tumor cells by macrophages in vitro, we tested the efficacy of anti-CD47 therapies for PanNETs in vivo. Twenty-five thousand APL1-GFP-Luc cells were injected orthotopically into the pancreases of NSG mice. Tumor-bearing mice were randomized into control or treatment groups based on luciferase activity (photons per s), which provides an accurate measure of cancer cell contribution to the mass. In one cohort, treatment was initiated 2 wk after tumor engraftment, whereas the second cohort began treatment 3 wk after engraftment. Tumor growth and response to treatment were monitored for 7 wk. In both the 2- and 3-wk engraftment cohorts, the anti-CD47 treatment groups had a significant reduction of tumor bioluminescence signal compared with the control groups, indicating inhibition of tumor growth (Fig. 3 *A* and *B*). In both engraftment cohorts, mice treated with anti-CD47 antibody also had significantly increased survival compared with mice treated with vehicle control (Fig. 3*C*). Gross inspection during necropsy showed that mice treated with anti-CD47 antibody lacked hepatic metastases, whereas mice treated with vehicle control had livers that were obliterated by tumor (Fig. S6*A*). The livers from mice treated with anti-CD47 antibody had no evidence of metastasis by light microscopy (Fig. S6*B*) or fluorescence microscopy (Fig. S6*D*). However, every liver from mice treated with vehicle control had diffuse, multilobar metastatic disease by light microscopy (Fig. S6*C*) and fluorescence microscopy (Fig. S6*E*).

We also tested the efficacy of anti-CD47 antibody therapy in a genetic PanNET mouse model created by deleting *Rb*, *p53*, and *p130* in insulin-producing cells (*RIP-Cre Rb/p53/p130*) (26). These mice develop pancreatic tumors within 2 wk after birth and die ∼2 mo after birth (26). We found that treatment of these mice with an anti-mouse CD47 antibody starting at day 35, when there is already a substantial tumor burden, significantly increased survival compared with mice treated with vehicle control (Fig. 3*D*).

We tested the efficacy of anti-CD47 antibody therapy in direct patient xenograft models using tumor 2. Thirty thousand tumor cells were injected s.c. into NSG mice and randomized into treatment or control cohorts. Tumors were allowed to grow for 1 wk before starting anti-CD47 treatment. Kaplan–Meier analysis revealed overall statistically increased survival of mice treated with anti-CD47 antibodies compared with mice treated with vehicle control (Fig. 3*E*). The details of this experiment are shown in *Supporting Information* (Fig. S6 *F–L*).

Anti-EGFR Therapies Combine with Anti-CD47 Therapy for Increased Anti-Tumor Activity. Because the treatments combining anti-CD47 and anti-EGFR monoclonal antibodies induced the phagocytosis of tumor cells by macrophages in vitro, we tested the efficacy of combination therapy for PanNETs in vivo. We injected 25,000 luciferase-labeled APL1 cells orthotopically into the pancreases of NSG mice. Treatment with PBS vehicle control, combination Hu5F9-G4 and cetuximab, or combination Hu5F9-G4 and panitumumab was initiated 2 wk after tumor engraftment. Tumor burden represented by fold-change in total photon flux (Fig. 3*F*) as measured by bioluminescence imaging for 4 wk was analyzed. Compared with PBS control, cetuximab alone and panitumumab alone did not significantly reduce tumor burden. However, compared with PBS control, Hu5F9-G4 significantly reduced tumor burden. Interestingly, combination of Hu5F9-G4 and either cetuximab or panitumumab reduced tumor burden more than any of the therapies alone.

Discussion

We began our study of PanNETs by performing an in-depth analysis of tumors at different stages in the disease process from a single patient who had previously exhausted all conventional

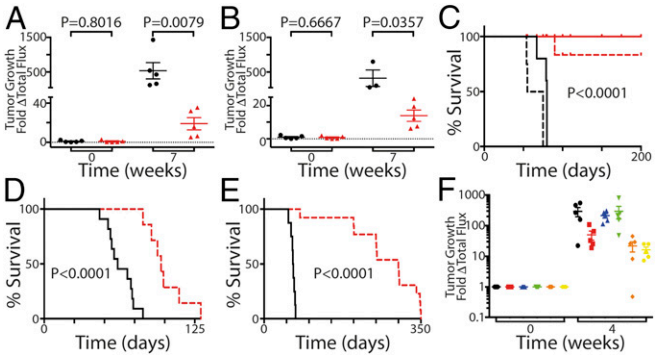

Fig. 3. Anti-CD47 therapy inhibits tumor growth and prolongs survival in vivo. Twenty-five thousand luciferase-labeled APL1 cells were injected orthotopically into the pancreases of NSG mice. Tumor-bearing mice were divided into control or treatment groups based on luciferase activity (photons per s). In one cohort, treatment with either anti-CD47 antibody (Hu5F9-G4) or PBS vehicle control was initiated 2 wk after tumor engraftment whereas, in a second cohort, treatment was initiated 3 wk after tumor engraftment. (*A* and *B*) Tumor burden represented by fold-change in total photon flux as measured by bioluminescence imaging for 7 wk was reduced following anti-CD47 therapy (Hu5F9-G4) in the treatment groups ($n = 5$; red) compared with the control groups ($n = 5$; black), indicating significant inhibition of tumor growth in both 2- ($P = 0.0079$) and 3-wk ($P = 0.0357$) engraftment cohorts. (*C*) Kaplan–Meier curve showing prolonged survival of mice treated with anti-CD47 antibody (Hu5F9-G4) in a 2-wk engraftment cohort ($n = 5$; solid red) and 3-wk engraftment cohort ($n = 5$; dashed red) compared with a carrier control 2-wk engraftment cohort ($n = 5$; solid black; median survival 80 d) ($P < 0.0001$) and 3-wk engraftment cohort ($n = 5$; dashed black; median survival 65 d) ($P < 0.0001$). (*D*) Kaplan–Meier curve showing prolonged survival of RIP-Cre Rb/p53/p130 mice treated with anti-CD47 antibody at postnatal day 35 (MIAP410) ($n = 8$; red; median survival 97 d) compared with carrier control ($n = 11$; black; median survival 61 d) ($P < 0.0001$). (*E*) Thirty thousand patient tumor cells injected s.c. into NSG mice, randomized into treatment or control cohorts, and treated after a 1-wk engraftment. Kaplan–Meier curve illustrating that mice from the control group ($n = 15$; black) ultimately died as a result of their tumors (median survival 64 d) but mice from the treatment group ($n = 15$; red) had prolonged survival ($P < 0.0001$). (*F*) Anti-EGFR therapies alone do not inhibit tumor growth, but anti-EGFR therapies may combine with anti-CD47 for increased antitumor activity. Twenty-five thousand luciferase-labeled APL1 cells were injected orthotopically into the pancreases of NSG mice. Tumor-bearing mice were divided into control or treatment groups based on luciferase activity (photons per s). Treatment with anti-CD47 antibody (Hu5F9-G4), anti-EGFR antibodies (cetuximab or panitumumab), combination Hu5F9-G4 and cetuximab, combination Hu5F9-G4 and panitumumab, or PBS vehicle control was initiated 2 wk after tumor engraftment and carried out for 4 wk. Tumor burdens represented by fold-change in total photon flux as measured by bioluminescence imaging were statistically different following Hu5F9-G4 therapy ($n = 5$; red), combination Hu5F9-G4 and cetuximab ($n = 5$; orange), and combination Hu5F9-G4 and panitumumab ($n = 5$; yellow) compared with the control group ($n = 5$; black), cetuximab therapy ($n = 5$; blue), and panitumumab therapy ($n = 5$; green). Means ± SEM.

therapies. Our analysis not only revealed potential therapeutic avenues for the patient in question but also illuminated fundamental biological processes for this class of tumors. Our examination of the index case and other patient PanNETs demonstrated the importance of MET activation for the growth of PanNETs, resulted in the development of PanNET models that will aid future studies of these tumors, and led to the identification of tumor-initiating cells. Additionally, it drove the validation of anti-CD47 therapy for inhibiting tumor growth, preventing metastatic disease, and prolonging survival.

Stem cells have the ability to generate large numbers of mature cells through a hierarchy of proliferation and differentiation while retaining the capacity to maintain the stem cell pool by continuous self-renewal. We and others have proposed that tumors consist of cells at various stages of differentiation, but all cells are derived from the same pool of self-renewing tumor-initiating cells that is ultimately responsible for the expansion and propagation of the tumor (5). Although the existence of neoplastic stem cells remains a controversial topic for some investigators (27, 28), several recent reports have used a variety of lineage-tracing techniques in experimental cancer models to conclusively demonstrate the existence of such a cellular hierarchy within tumors (29). Our results reveal that CD90 expression marks a subset of tumor-initiating cells within PanNETs. CD90 is a marker of transplantable mouse and human hematopoietic stem cells (20), and has also been described as a tumor-initiating cell marker in a number of cancers (9, 21). Very little is currently known about CD90 signaling capabilities, and potential ligands are poorly characterized. Thus, elucidating the functional mechanisms by which CD90 contributes to cancer and stem cell biology will be a primary aim of our future studies.

A major challenge in identifying tumorigenic cells in well-differentiated PanNETs is efficiently generating tumor xenografts in mouse models. Of the 39 WHO grade 1 and 2 primary patient PanNETs that we transplanted into immunodeficient mice (Dataset S1), only 1 tumor (tumor 2; Dataset S1) developed into xenografts without the aid of MET agonists and with high efficiency and reproducibility. This is in contrast to our experience with pancreatic ductal adenocarcinoma, for which we collected 39 primary patient tumor samples and generated 24 xenografts. Other researchers have experienced similar difficulties in transplanting and growing low- and intermediate-grade PanNETs in mice (23). The difficulty of growing well-differentiated PanNET xenografts may be attributed to the lack of specific human growth factors in recipient mice. Gene expression profiling of patient tumor samples and functional studies on tumor xenografts revealed that MET signaling is a key regulator of PanNET growth. Others have found that MET is a principal regulator of tumor aggressiveness of PanNETs in mice and human cell lines (19). Aberrant expression of MET has been observed in many solid tumors, yet most rely on activation of MET signaling by HGF (30). Mouse HGF is unable to activate human MET (31–33), thereby limiting the growth of HGF-dependent human tumors. Our results suggest that only tumors that express HGF, and therefore can stimulate MET in an autocrine fashion, are capable of growing in environments devoid of exogenous HGF. Thus, an alternative mouse model, particularly one that produces human HGF, may be required to facilitate the growth of PanNET xenografts for the majority of tumors. Furthermore, our findings indicate that disruption of MET signaling via blocking antibodies or proteins directed against either ligand (HGF) or receptor (MET) may be a viable therapeutic option for the treatment of PanNETs in humans. The functional significance of MET signaling for tumor initiation and metastasis as well as the efficacy of anti-MET therapies for the treatment of PanNETs should be subjects of further investigations.

A key impediment in the study of the biology of PanNETs and the development of new therapies for these tumors is the lack of well-validated, representative experimental models. As part of this study, we developed a cell line derived from a well-differentiated patient PanNET (tumor 2). The APL1 cell line expresses both MET and HGF, allowing for autocrine MET stimulation. This further supports our hypothesis that MET stimulation, through exogenous, paracrine, or autocrine signaling, is required for tumor growth. More importantly, this discovery provides a critically needed model of PanNETs with which to perform additional studies.

We previously reported that tumor cells that overexpress CD47 protect themselves from macrophage-mediated destruction (34). We now extend these findings to PanNET cells and demonstrate that blocking anti-CD47 agents enables macrophages to ingest PanNET cells that were otherwise exempt from destruction. Moreover, anti-CD47 blocking antibodies inhibited the growth of PanNETs, prevented metastatic disease, and dramatically improved survival in a genetic model and xenograft assays. CD47 is expressed on all tumor cells, and the expression of CD47 is increased in the tumor-initiating cell population. Thus, anti-CD47 therapy not only targets the critical tumor-initiating cell population, whose elimination

is required for tumor eradication, but also the bulk cells of the tumor. Our group has developed humanized anti-CD47 monoclonal antibodies for patients with solid and hematologic malignancies, and phase 1 clinical trials have been initiated. These results provide a strong preclinical justification for testing blocking anti-CD47 antibodies in patients with PanNETs.

We tested the efficacy of dual targeting of CD47 and EGFR on PanNETs. EGFR is highly expressed on the surface of most PanNET cells tested. Interestingly, we found that anti-EGFR therapy alone with either cetuximab or panitumumab did not inhibit tumor growth. Anti-CD47 therapy with Hu5F9-G4 significantly reduced tumor growth, which is consistent with our previous results. However, combination of anti-CD47 therapy with anti-EGFR therapy inhibited tumor growth to a greater degree than either therapy alone. Thus, we are hopeful that dual targeting of CD47 with PanNET-specific antigens will provide clinically significant benefits for patients with PanNETs.

Starting with a multidisciplinary analysis of a single patient's tumor, an integrative approach resulted in a number of significant discoveries. First, we established in primary patient tumors that paracrine activation of MET is essential for the growth of PanNETs. We also identified the tumor-initiating cell population in PanNETs and genes that differentiate the tumor-initiating cells from bulk tumor cells. Moreover, we demonstrated the efficacy of anti-CD47 therapy in this tumor type using cell lines, genetic mouse models, and patient-derived tumor xenografts. Finally, we generated a reproducible xenograft model and a cell line from a human PanNET that will aid in the study of this poorly understood cancer. Our hope is that these findings will provide additional tools for further study of PanNETs and an approach for prioritizing treatment options and ultimately improving survival for patients with PanNETs.

Materials and Methods

The study used 39 well-differentiated, WHO grade 1 and 2 human PanNET specimens sequentially obtained from consented patients undergoing surgical resection at Stanford Hospital as approved by the Stanford University Institutional Review Board Panel on Medical Human Subjects (protocol 22185) to characterize fundamental biological features, identify tumorigenic cells, and identify potential therapeutic targets for PanNETs. All animal handling, surveillance, and experimentation were performed in accordance with and approval from the Stanford University Administrative Panel on Laboratory Animal Care (protocol 26270). For all in vivo experiments, mice were randomly assigned to either the vehicle control or the treatment group. The details of the materials and methods are shown in *SI Materials and Methods*.

ACKNOWLEDGMENTS. We recognize the important contributions of Theresa A. Storm, Anne K. Volkmer, Norma F. Neff, Benedetto Passarelli, Hanlee P. Ji, Ingrid Ibarra, Rahul Sinha, Siddhartha S. Mitra, Stephen R. Quake, Humberto Contreras-Trujillo, Tejaswitha Naik, Aaron McCarty, Charlene Wang, Libuse Jerabek, Sanjiv S. Gambhir, Xinrui Yan, Laura J. Pisani, and Timothy C. Doyle to this project. This project was funded by the Virginia and D. K. Ludwig Fund for Cancer Research, an anonymous donors fund, National Cancer Institute (P01 CA139490), Siebel Stem Cell Institute and Thomas and Stacey Siebel Foundation, an A. P. Giannini Foundation Postdoctoral Research Fellowship in California, an American College of Surgeons Resident Research Scholarship, an Advanced Residency Training at Stanford (ARTS) Fellowship, and a Howard Hughes Medical Institute Medical Research Fellowship.

1. Rindi G, Wiedenmann B (2012) Neuroendocrine neoplasms of the gut and pancreas: New insights. *Nat Rev Endocrinol* 8(1):54–64.
2. Yao JC, et al.; RAD001 in Advanced Neuroendocrine Tumors, Third Trial (RADIANT-3) Study Group (2011) Everolimus for advanced pancreatic neuroendocrine tumors. *N Engl J Med* 364(6):514–523.
3. Raymond E, et al. (2011) Sunitinib malate for the treatment of pancreatic neuroendocrine tumors. *N Engl J Med* 364(6):501–513.
4. Krampitz GW, Norton JA (2013) Pancreatic neuroendocrine tumors. *Curr Probl Surg* 50(11):509–545.
5. Reya T, Morrison SJ, Clarke MF, Weissman IL (2001) Stem cells, cancer, and cancer stem cells. *Nature* 414(6859):105–111.
6. Lapidot T, et al. (1994) A cell initiating human acute myeloid leukaemia after transplantation into SCID mice. *Nature* 367(6464):645–648.
7. Al-Hajj M, Wicha MS, Benito-Hernandez A, Morrison SJ, Clarke MF (2003) Prospective identification of tumorigenic breast cancer cells. *Proc Natl Acad Sci USA* 100(7):3983–3988.
8. Li C, et al. (2007) Identification of pancreatic cancer stem cells. *Cancer Res* 67(3):1030–1037.
9. Yang ZF, et al. (2008) Significance of $CD90^+$ cancer stem cells in human liver cancer. *Cancer Cell* 13(2):153–166.
10. Prehn RT (1972) The immune reaction as a stimulator of tumor growth. *Science* 176(4031):170–171.
11. Chao MP, Majeti R, Weissman IL (2012) Programmed cell removal: A new obstacle in the road to developing cancer. *Nat Rev Cancer* 12(1):58–67.
12. Willingham SB, et al. (2012) The CD47-signal regulatory protein alpha (SIRPa) interaction is a therapeutic target for human solid tumors. *Proc Natl Acad Sci USA* 109(17):6662–6667.
13. Chao MP, et al. (2010) Anti-CD47 antibody synergizes with rituximab to promote phagocytosis and eradicate non-Hodgkin lymphoma. *Cell* 142(5):699–713.
14. Weiskopf K, et al. (2013) Engineered SIRPα variants as immunotherapeutic adjuvants to anticancer antibodies. *Science* 341(6141):88–91.
15. Tseng D, et al. (2013) Anti-CD47 antibody-mediated phagocytosis of cancer by macrophages primes an effective antitumor T-cell response. *Proc Natl Acad Sci USA* 110(27):11103–11108.
16. Sahoo D, Dill DL, Gentles AJ, Tibshirani R, Plevritis SK (2008) Boolean implication networks derived from large scale, whole genome microarray datasets. *Genome Biol* 9(10):R157.
17. Peruzzi B, Bottaro DP (2006) Targeting the c-Met signaling pathway in cancer. *Clin Cancer Res* 12(12):3657–3660.
18. Zhang YW, et al. (2010) MET kinase inhibitor SGX523 synergizes with epidermal growth factor receptor inhibitor erlotinib in a hepatocyte growth factor-dependent fashion to suppress carcinoma growth. *Cancer Res* 70(17):6880–6890.
19. Sennino B, et al. (2012) Suppression of tumor invasion and metastasis by concurrent inhibition of c-Met and VEGF signaling in pancreatic neuroendocrine tumors. *Cancer Discov* 2(3):270–287.
20. Spangrude GJ, Heimfeld S, Weissman IL (1988) Purification and characterization of mouse hematopoietic stem cells. *Science* 241(4861):58–62.
21. Salcido CD, Larochelle A, Taylor BJ, Dunbar CE, Varticovski L (2010) Molecular characterisation of side population cells with cancer stem cell-like characteristics in small-cell lung cancer. *Br J Cancer* 102(11):1636–1644.
22. Laird DJ, De Tomaso AW, Weissman IL (2005) Stem cells are units of natural selection in a colonial ascidian. *Cell* 123(7):1351–1360.
23. Gaur P, et al. (2011) Identification of cancer stem cells in human gastrointestinal carcinoid and neuroendocrine tumors. *Gastroenterology* 141(5):1728–1737.
24. Hu Y, Smyth GK (2009) ELDA: Extreme limiting dilution analysis for comparing depleted and enriched populations in stem cell and other assays. *J Immunol Methods* 347(1-2):70–78.
25. Chao MP, et al. (2011) Therapeutic antibody targeting of CD47 eliminates human acute lymphoblastic leukemia. *Cancer Res* 71(4):1374–1384.
26. Jahchan NS, et al. (2013) A drug repositioning approach identifies tricyclic antidepressants as inhibitors of small cell lung cancer and other neuroendocrine tumors. *Cancer Discov* 3(12):1364–1377.
27. Quintana E, et al. (2010) Phenotypic heterogeneity among tumorigenic melanoma cells from patients that is reversible and not hierarchically organized. *Cancer Cell* 18(5):510–523.
28. Boiko AD, et al. (2010) Human melanoma-initiating cells express neural crest nerve growth factor receptor CD271. *Nature* 466(7302):133–137.
29. Schepers AG, et al. (2012) Lineage tracing reveals $Lgr5^+$ stem cell activity in mouse intestinal adenomas. *Science* 337(6095):730–735.
30. Christensen JG, Burrows J, Salgia R (2005) c-Met as a target for human cancer and characterization of inhibitors for therapeutic intervention. *Cancer Lett* 225(1):1–26.
31. Jeffers M, Rong S, Vande Woude GF (1996) Hepatocyte growth factor/scatter factor-Met signaling in tumorigenicity and invasion/metastasis. *J Mol Med (Berl)* 74(9):505–513.
32. Rong S, et al. (1992) Tumorigenicity of the met proto-oncogene and the gene for hepatocyte growth factor. *Mol Cell Biol* 12(11):5152–5158.
33. Sonnenberg E, Meyer D, Weidner KM, Birchmeier C (1993) Scatter factor/hepatocyte growth factor and its receptor, the c-met tyrosine kinase, can mediate a signal exchange between mesenchyme and epithelia during mouse development. *J Cell Biol* 123(1):223–235.
34. Jaiswal S, et al. (2009) CD47 is upregulated on circulating hematopoietic stem cells and leukemia cells to avoid phagocytosis. *Cell* 138(2):271–285.
35. Trapnell C, et al. (2012) Differential gene and transcript expression analysis of RNA-seq experiments with TopHat and Cufflinks. *Nat Protoc* 7(3):562–578.
36. Anders S, Huber W (2010) Differential expression analysis for sequence count data. *Genome Biol* 11(10):R106.
37. Trapnell C, et al. (2010) Transcript assembly and quantification by RNA-Seq reveals unannotated transcripts and isoform switching during cell differentiation. *Nat Biotechnol* 28(5):511–515.
38. Subramanian A, et al. (2005) Gene set enrichment analysis: a knowledge-based approach for interpreting genome-wide expression profiles. *Proc Natl Acad Sci USA* 102(43):15545–15550.
39. Li H, Durbin R (2009) Fast and accurate short read alignment with Burrows-Wheeler Transform. *Bioinformatics* 25(14):1754–1760.
40. Li H, et al. (2009) The Sequence alignment/map (SAM) format and SAMtools. *Bioinformatics* 25(16):2078–2079.
41. Rosset A, Spadola L, Ratib O (2004) OsiriX: an open-source software for navigating in multidimensional DICOM images. *J Digit Imaging* 17(3):205–216.
42. Kim MP, et al. (2009) Generation of orthotopic and heterotopic human pancreatic cancer xenografts in immunodeficient mice. *Nat Protoc* 4(11):1670–1680.